$Mo_{4-x}Fe_x$ nanoalloy: Structural transition and electronic structure of interest in spintronics

A. García-Fuente and A. Vega
Departamento de Física Teórica, Atómica, y Óptica, Universidad de Valladolid, E-47011 Valladolid, Spain

F. Aguilera-Granja
Instituto de Física, Universidad Autónoma de San Luis Potosí, San Luis Potosí, 78000 Mexico

L. J. Gallego
Departamento de Física de la Materia Condensada, Facultad de Física, Universidad de Santiago de Compostela, E-15706 Santiago de Compostela, Spain

(Received 12 December 2008; revised manuscript received 23 February 2009; published 4 May 2009)

A systematic *ab initio* study of the structures and magnetic properties of $Mo_{4-x}Fe_x$ clusters ($x=1-3$) is reported. The linear structure of Mo_4 remains stable upon substitutional doping by one and even two Fe atoms, above which a transition to the tetrahedral geometry of pure Fe_4 takes place. The cluster Mo_2Fe_2 is particularly interesting since, among the rich variety of isomers of different dimensionalities and magnetic orders, its ground state and first-excited state essentially differ in the magnetic coupling between the two Fe atoms across a tightly bound Mo dimer. The equivalent to the interlayer exchange coupling observed in sandwiches and multilayers is determined in this molecular magnet, whose electronic structure makes it a good candidate to be used either as a field sensor or as a spin valve in molecular spintronics.

DOI: 10.1103/PhysRevB.79.184403 PACS number(s): 36.40.Cg, 31.15.A−, 61.46.Bc, 75.75.+a

I. INTRODUCTION

One of the questions of major technological interest at present is the production and control of molecular magnets to be used in nanodevices for molecular spintronics.[1,2] Quantum confinement effects produced at the nanoscale level are expected to open new possibilities beyond those already achieved in the last two decades when, for instance, the interlayer exchange coupling (IEC) (Refs. 3 and 4) and the giant magnetoresistance (GMR) (Refs. 5 and 6) were discovered in extended systems such as superlattices and multilayers. In this context, new prospects are expected for improving the performance of the magnetoresistive read heads in magnetic recording and storage devices.

The magnetic properties of free one-component clusters of transition-metal (TM) atoms have been widely investigated by experimental and theoretical methods. Free atomic clusters have been produced by pulsed laser vaporization, among other methods, and their magnetic moments have been determined by Stern-Gerlach-type deflection experiments.[7,8] Most theoretical investigations have been performed using the tight-binding method (see, e.g., Ref. 9) or *ab initio* methods based on density-functional theory (DFT) with different implementations (all electron or pseudopotentials, plane waves or pseudoatomic orbitals, different approximations for the exchange and correlation, etc.). In contrast, the magnetic properties of binary clusters of TM atoms, which are the nanometric equivalent to bulk alloys, have received less attention, although a significant number of studies have recently been performed.[10–12] Binary clusters of TM atoms are of special interest not only for theoretical reasons but also for their possible application as magnetic recording media. The main theoretical difficulty to deal with this kind of cluster relies on the fact that TM atoms include both relatively localized *d* electrons and relatively delocalized *sp* electrons. For binary clusters of TM atoms one can follow a similar strategy as in the case of magnetic multilayered systems or bulk alloys, trying to take advantage of the magnetic properties of the selected constituent elements together with the cooperative effects, in order to find customized molecular magnets with interesting behaviors.

Cr and Mo are unique among the TMs. Their half-filled electronic configurations result in strong *d-d* bonding in the dimers with exceptional short bonds (1.68 Å for Cr_2 and 1.93 Å for Mo_2,[13] while the bulk interatomic distances are 2.50 and 2.73 Å, respectively). The exceptionally strong *d-d* interactions in the dimers dictates the growth and structures of small Cr and Mo clusters, which have been studied by DFT methods (see, e.g., Refs. 14–18). In particular, for Mo_n clusters ($n=2-13$), recent calculations using the SIESTA code[19] with the generalized gradient approximation (GGA) have shown that linear [one-dimensional (1D)], planar [two-dimensional (2D)], and three-dimensional (3D) clusters have a strong tendency to form dimers.[18] In general, even-numbered Mo clusters are more stable than their neighboring odd-numbered clusters because they can accommodate an integer number of tightly bound dimers. As a consequence, the binding energies of Mo clusters exhibit, in their lowest-energy states, an odd-even effect in all dimensionalities, and the even-numbered Mo clusters have quenched magnetic moments.[18]

In the present work we have performed a systematic study of the effect of substitutional doping a 1D Mo cluster such as Mo_4, which has two tightly bound dimers, by Fe atoms which are expected to have large magnetic moments and parallel magnetic coupling when placed at nearest-neighbor positions. Since Fe_4 has a tetrahedral 3D ground-state geometry,[16] an 1D-3D structural transition is expected in $Mo_{4-x}Fe_x$ clusters when x is increased, i.e., when Mo_4 is doped by a sufficient number of Fe atoms. We will show here

that among the rich variety of isomers of different dimensionalities and magnetic orders of Mo_2Fe_2, the linear cluster is particularly interesting as regards the magnetic couplings between the two Fe atoms across a Mo dimer which acts as a spacer, like in magnetic multilayers in which the IEC can be determined and related with magnetoresistance (MR) effects. The electronic structure of this cluster makes it a candidate to be used either as a field sensor or as a spin valve in molecular spintronics.

The essential technical details of the computations performed in this paper are described below in Sec. II. In Sec. III we present and discuss our results and in Sec. IV we summarize our main conclusions.

II. DETAILS OF THE COMPUTATIONAL PROCEDURE

Our calculations were performed using the *ab initio* DFT-based code SIESTA,[19] with the additional noncollinear (NCL) GGA implementation by García-Suárez *et al.*[20] (the GGA functional as parameterized by Perdew *et al.*[21]). The atomic cores were replaced by nonlocal norm-conserving pseudopotentials.[22] We included nonlinear core corrections to account for the significant overlap of the semicore and valence *d* states. Valence states were described by triple ζ doubly polarized basis sets. The clusters were placed in cubic boxes with a lateral size of 20 Å, which are big enough to have negligible electric fields at their edges. We used an energy cutoff of 200 Ry to describe the finite real-space grid for numerical calculations involving the electron density. Using a conjugate gradient method, the atomic and electronic degrees of freedom of the clusters were allowed to relax simultaneously and self-consistently until interatomic forces were smaller than 0.001 eV/Å. As starting geometries we used all possibilities for a four-atoms cluster, and as starting magnetic structures the possible collinear inputs of ferromagnetic (FM) and antiferromagnetic (AFM) types, as well as NCL configurations. The forces on ions were computed using a variant of the Hellmann-Feynman theorem that includes Pulay-type corrections to take into account the fact that the basis sets are not complete and move with the atoms.[19] The spin-orbit interactions were not taken into account in our calculations because they have little influence on the magnetic properties of 3*d* and 4*d* TM clusters.[23]

III. RESULTS

Figure 1 shows the lowest-energy isomers of Mo_3Fe that were identified in our calculations using SIESTA-GGA, with their relative energies and total and atomic magnetic moments, μ and μ_{at}. The corresponding bond lengths d_{ij} are listed in Table I. All the isomers of Mo_3Fe have collinear (CL) magnetic order. The most stable isomer, which has a 1D structure and FM order, is formed by a Mo and an Fe atom separated by a Mo dimer with quenched magnetic moment. This is due to the pairing of the *d* electrons so that only the *s* electrons contribute to its magnetic moment. The other Mo atom has a large magnetic moment close to its saturation, which is produced by nearly 5 unpaired *d* electrons and some *s* contribution. The Fe atom of the most stable Mo_3Fe isomer has a large magnetic moment mainly due to the *d* electrons and the total magnetic moment of this isomer is $8\mu_B$. The next most stable isomer, nearly degenerated with the ground state (the difference in energy is only 2 meV), is a spin

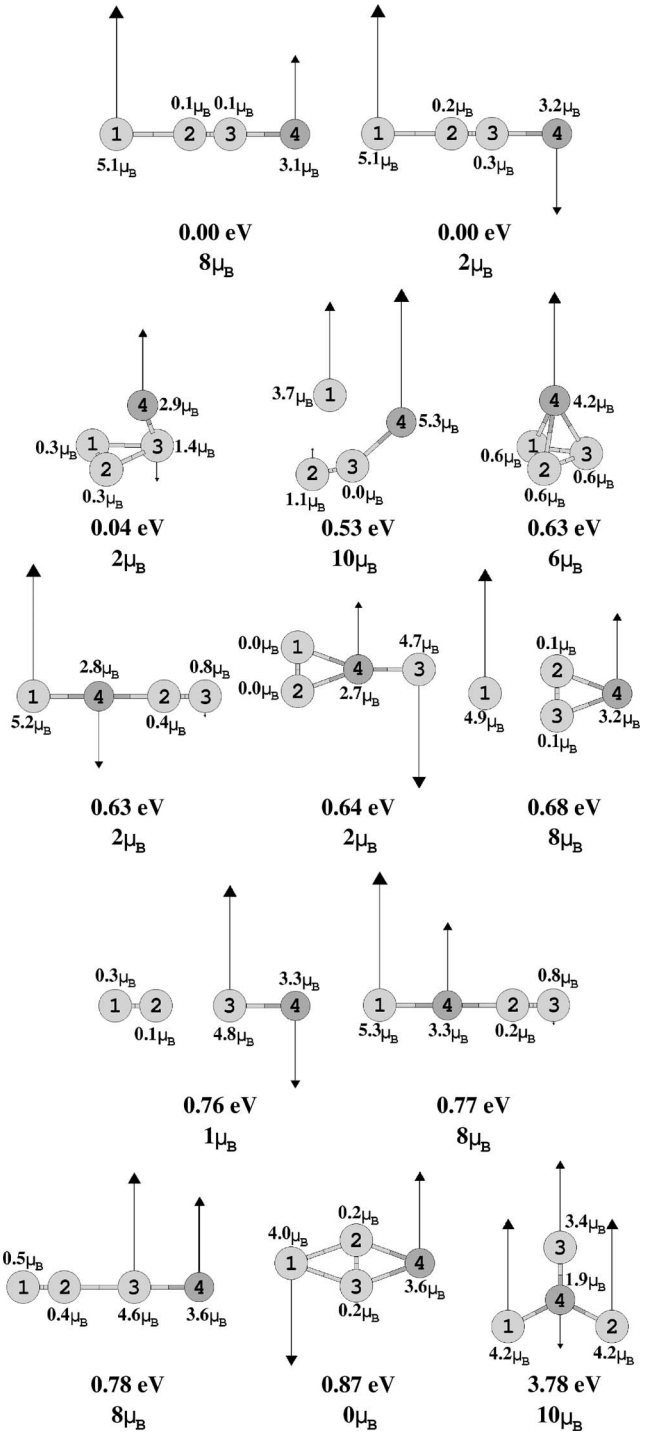

FIG. 1. Predicted lowest-energy isomers of Mo_3Fe with their relative energies and absolute values of the total and atomic magnetic moments. Dark gray spheres represent Fe atoms and light gray spheres represent Mo atoms. The arrows indicate the directions and magnitudes of the atomic magnetic moments (some Mo magnetic moments are 0 or very small to be appreciated in the figure). Numbers on atoms are used to refer to these atoms in Table I.

TABLE I. Relative energies, dimensionalities, and bond lengths of the lowest-energy isomers of Mo_3Fe.

ΔE	Dim.	d_{12}	d_{13}	d_{14}	d_{23}	d_{24}	d_{34}
0.00	1D	2.88	4.46	7.01	1.58	4.13	2.55
0.00	1D	2.90	4.48	7.03	1.58	4.13	2.55
0.04	3D	1.88	2.56	2.85	2.56	2.85	2.06
0.53	2D	3.20	2.92	3.01	1.61	4.05	2.57
0.63	3D	2.21	2.21	2.67	2.21	2.67	2.67
0.63	1D	5.15	6.76	2.58	1.61	2.57	4.18
0.64	2D	1.74	4.85	2.53	4.85	2.53	2.39
0.68	2D	2.96	2.96	5.19	1.76	2.52	2.52
0.76	1D	1.61	4.54	7.13	2.93	5.51	2.58
0.77	1D	5.25	6.86	2.68	1.60	2.57	4.18
0.78	1D	1.61	4.39	6.95	2.78	5.34	2.56
0.87	2D	2.71	2.71	5.05	1.80	2.65	2.65
3.78	2D	4.08	3.71	2.30	3.71	2.30	2.05

isomer with AFM (or, more precisely, ferrimagnetic-like) order. It has similar atomic arrangement and local atomic moments as the ground state but the total magnetic moment is $2\mu_B$. The third lowest-lying isomer, which is only 35 meV less stable than the ground state, has also two tightly bound Mo atoms of very small magnetic moments, AFM order, and $\mu=2\mu_B$ but it is 3D. We identified ten more Mo_3Fe isomers that have 2D/FM, 3D/FM, 1D/AFM, 2D/AFM, 2D/FM, 1D/AFM, 1D/FM, 1D/FM, 2D/AFM, and 2D/AFM dimensionalities/magnetic orders, respectively (in increasing order of energies), all of which are much less stable than the ground state.

Figure 2 and Table II show our results for Mo_2Fe_2. All the isomers of Mo_2Fe_2 have also CL magnetic order. The most stable isomer of this cluster is predicted to have a 1D geometry with a tightly bound Mo dimer in the center and an Fe atom at each end. The coupling between the magnetic moments of the Fe atoms through the Mo dimer is AFM. The next most stable isomer, nearly equienergetic with the ground state, is a spin isomer with FM coupling and absolute values of the atomic magnetic moments similar to those of the ground state. The third lowest-lying isomer (250 meV less stable than the ground state) has a 2D geometry of rhomboidal shape, with a Mo dimer placed at transversal position, the total magnetic moment being $0\mu_B$ due to the AFM coupling. The remaining six identified Mo_2Fe_2 isomers have 1D/FM, 3D/FM, 2D/FM, 1D/AFM, 2D/AFM, and 2D/AFM dimensionalities/magnetic orders, respectively.

The information about the predicted lowest-energy isomers of $MoFe_3$ is shown in Fig. 3 and Table III. At the composition corresponding to $MoFe_3$, a 1D–3D structural transition occurs. The most stable isomer of $MoFe_3$ has a 3D geometry of tetrahedral type (which is the geometry of Fe_4; Ref. 16), AFM order, a Mo magnetic moment of $0\mu_B$ and a total magnetic moment of $4\mu_B$. The next most stable isomer, whose energy is not very far from that of the ground state, has also tetrahedral geometry, but, unlike in the ground state, the coupling within the Fe_3 subcluster is FM, giving rise to a cluster magnetic moment of $10\mu_B$. Because this is the magnetic coupling in the triangular ground state of Fe_3,[16] our results indicate that the presence of the Mo atom in the proximity of Fe_3 produces, after full relaxation, a strong modification of the Fe-Fe magnetic coupling. In the ground state of $MoFe_3$, two Fe atoms [Fe(2) and Fe(3) in Fig. 3] are very close to each other and relatively far from the remaining Fe atom (the corresponding distances are shown in Table III). This separation between one Fe atom and the other two Fe atoms is detrimental for FM coupling in the Fe subcluster. The third lowest-lying isomer of $MoFe_3$ is also a spin isomer of tetrahedral geometry, which has AFM coupling and a total magnetic moment of $2\mu_B$. The triangular structure adopted

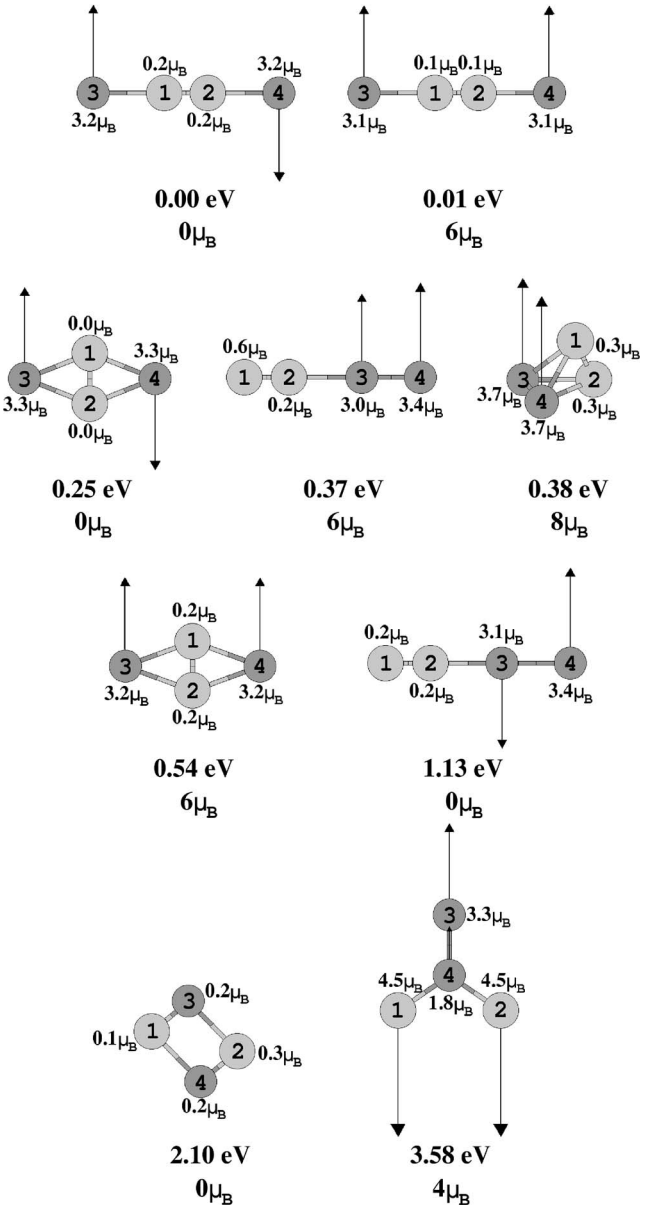

FIG. 2. Predicted lowest-energy isomers of Mo_2Fe_2 with their relative energies and absolute values of the total and atomic magnetic moments. Dark gray spheres represent Fe atoms and light gray spheres represent Mo atoms. The arrows indicate the directions and magnitudes of the atomic magnetic moments (some Mo magnetic moments are 0 or very small to be appreciated in the figure). Numbers on atoms are used to refer to these atoms in Table II.

TABLE II. Relative energies, dimensionalities, and bond lengths of the lowest-energy isomers of Mo_2Fe_2.

ΔE	Dim.	d_{12}	d_{13}	d_{14}	d_{23}	d_{24}	d_{34}
0.00	1D	1.57	2.55	4.13	4.13	2.55	6.68
0.01	1D	1.57	2.55	4.13	4.13	2.55	6.68
0.25	2D	1.83	2.52	2.52	2.52	2.52	4.69
0.37	1D	1.60	4.23	6.33	2.62	4.73	2.11
0.38	3D	1.79	2.69	2.59	2.59	2.70	2.44
0.54	2D	1.77	2.58	2.58	2.58	2.58	4.84
1.13	1D	1.62	4.18	6.65	2.57	5.03	2.46
2.10	2D	3.15	1.71	2.52	2.51	1.71	2.93
3.58	2D	3.70	3.91	2.25	3.91	2.25	2.17

by the Fe subcluster together with the magnetic coupling with the neighboring Mo atom leads to a competition between FM and AFM order in Fe, which may trigger the stabilization of NCL magnetic configurations in such structure. We note that this FM-AFM competition is not of the same type as that occurring in small clusters of AFM metals such as Mn, in which the geometries imposed by the dominant nonmagnetic interactions frustrate the adoption of fully AFM configurations (see, e.g., Refs. 24–27). We have identified, as the fourth lowest-lying isomer of $MoFe_3$, a NCL tetrahedral isomer with a net magnetic moment of $0\mu_B$. At larger energies, we found four 2D isomers: an AFM isomer with $\mu=0\mu_B$, an AFM isomer with $\mu=4\mu_B$, a FM isomer with $\mu=7\mu_B$, and a NCL isomer with $\mu=0\mu_B$ in which the Fe atoms also form a triangle. At even much larger energies, we found two 1D isomers, which are energetically less favorable due to the relatively high concentration of Fe, with AFM and FM coupling, respectively.

The ground state and the second lowest-lying isomer of Mo_2Fe_2 (considerably more stable than the other isomers of the same stoichiometry, as indicated above) are particularly interesting as regard to the exchange coupling (AFM or FM) between their Fe atoms across the nearly nonmagnetic tightly bound Mo dimer, which acts as a spacer. This situation can be seen as the 1D atomic limit of the IEC (Refs. 3 and 4) observed in magnetic sandwiches and multilayers to which the MR effects were directly related.[5,6] Recently, [Fe(1.5 nm)/Mo(t nm)] multilayers were prepared by electron-beam evaporation.[28] AFM interlayer coupling between the Fe slabs across the nonmagnetic Mo spacer was observed, like in our Mo_2Fe_2 cluster (Fig. 2). The spin-dependent scattering at the interfaces was shown to be relevant for the negative MR of multilayers with $t<3$ nm. The MR curve was saturated at low-magnetic fields with small MR ratio (less than 0.4%), as a consequence of which the field sensitivity, one of features of major technological interest, was not quite big. In analogy to the IEC in magnetic multilayers, we can estimate the exchange coupling across the Mo dimer (the spacer here) to be $\Delta E=E_{\mathrm{FM}}-E_{\mathrm{AFM}}=10$ meV, which corresponds to the energy difference between the second lowest-lying isomer and the ground state of Mo_2Fe_2 (see Fig. 2).

In order to see whether these 1D nanomagnets could be relevant in molecular spintronics and to understand how the

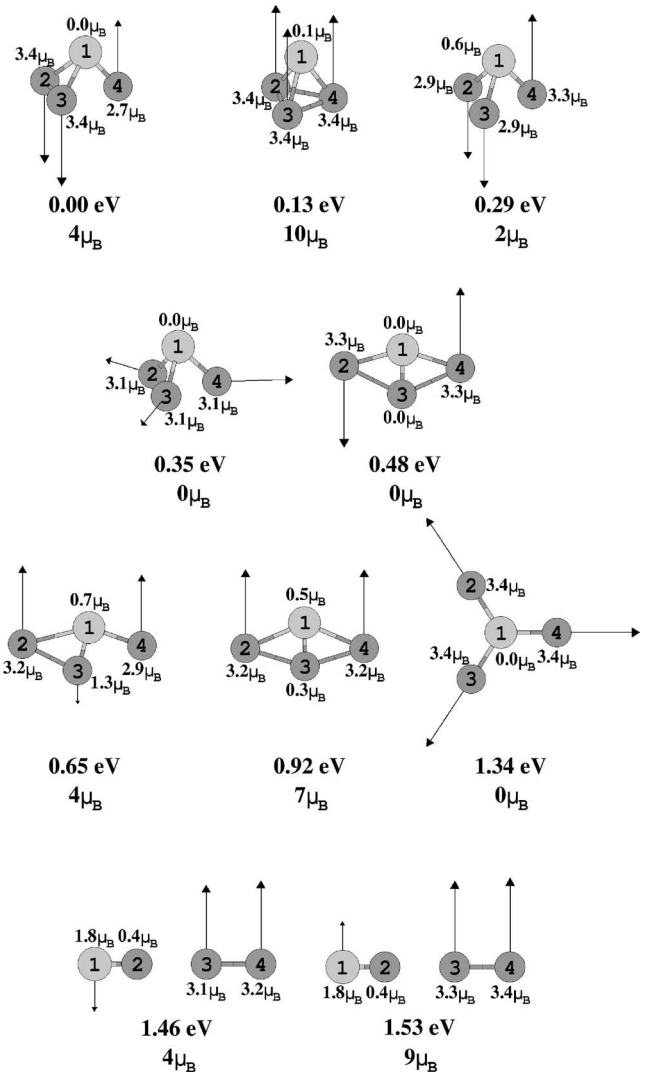

FIG. 3. Predicted lowest-energy isomers of $MoFe_3$ with their relative energies and absolute values of the total and atomic magnetic moments. Dark gray spheres represent Fe atoms and light gray spheres represent Mo atoms. The arrows indicate the directions and magnitudes of the atomic magnetic moments (some Mo magnetic moments are 0 or very small to be appreciated in the figure). Numbers on atoms are used to refer to these atoms in Table III.

confinement effects due to the finite size are reflected in the magnetic properties as compared with their multilayer counterparts, we have analyzed in detail their electronic structure. Figures 4 and 5 show the spin and orbital projected electronic densities of states for the ground state and the second lowest-lying isomer of Mo_2Fe_2, respectively. The highest occupied molecular orbital (HOMO) and the lowest unoccupied molecular orbital (LUMO) are expected to be the main states involved in the conductance of the cluster when anchored to the leads at low-bias voltage.[29] The HOMO in the ground state AFM configuration is located about 0.30 eV below the Fermi level (E_F); it has both majority and minority-spin components and the d character of Fe with a small p contribution of Mo. The LUMO is located 0.30 eV above E_F; it has also both majority and minority-spin components but only pure d character. In the FM configuration,

TABLE III. Relative energies, dimensionalities, and bond lengths of the lowest-energy isomers of $MoFe_3$.

ΔE	Dim.	d_{12}	d_{13}	d_{14}	d_{23}	d_{24}	d_{34}
0.00	3D	2.31	2.31	2.08	2.36	2.99	2.94
0.13	3D	2.32	2.37	2.33	2.44	2.46	2.43
0.29	3D	2.27	2.27	2.13	2.65	2.70	2.69
0.35	3D	2.20	2.21	2.21	2.77	2.75	2.71
0.48	2D	2.44	1.80	2.44	2.59	4.67	2.57
0.65	2D	2.76	1.80	2.24	2.46	4.79	2.77
0.92	2D	2.60	1.76	2.60	2.50	4.78	2.50
1.34	2D	2.22	2.22	2.26	3.75	3.92	3.92
1.46	1D	1.62	4.28	6.38	2.67	4.76	2.10
1.53	1D	1.62	4.31	6.43	2.69	4.81	2.12

corresponding to the second lowest-lying isomer, the situation is different. The HOMO is now located about 0.25 eV below E_F; it has the *d* character of Fe with a small *p* contribution of Mo but, in contrast to the AFM configuration, it has a pure minority-spin component. The LUMO is located 0.30 eV above E_F, it is of pure *d* character and also has minority-spin component only.

If we consider the axial direction as the direction of the electronic conduction when these clusters are connected at each end with a source and a drain lead, respectively, the electronic scattering will depend, as in the multilayers case, on the magnetic coupling between the Fe atoms across the Mo dimer. The spin-resolved charge densities for the HOMO and LUMO states of the AFM and FM configurations of Mo_2Fe_2 are shown in Figs. 4 and 5, respectively. In the AFM configuration, the HOMO and LUMO majority charge densities are located mainly around one of the Fe ends, whereas the minority charge densities are located around the other Fe end. The Mo states are polarized due to the hybridization with Fe. In the FM configuration the situation is different: there is no majority charge density at all in the system and the minority charge density is more noticeable around both Fe sites. In the electronic transport through the FM configuration of Mo_2Fe_2, the majority-spin electrons will suffer a strong scattering and, therefore, this molecular magnet should act as a spin valve. In the AFM configuration, the conduction of electrons with a spin component will be similar to the other and their resistivity will be greater than for the minority-spin electrons in the FM configuration. This opens the possibility of enhancing the MR ratio. The possibility of tuning the magnetic coupling through an external magnetic field would provide a mean to modify the conductance of the device across the molecular magnet, which could serve either as a field sensor or as a spin valve. We note that the functionality of these molecular magnets will also depend on the source and drain electrodes to which they can be connected. The relocation of the HOMO and LUMO molecular states with respect to the Fermi level of the electrodes, as well as the degree of hybridization between these states and the conduction band of the electrodes, are of fundamental importance for the kind of electronic conduction in the system.

IV. CONCLUSIONS

Our *ab initio* DFT-based study of $Mo_{4-x}Fe_x$ clusters ($x=1-3$) predicts the linear structure of Mo_4 to be stable upon

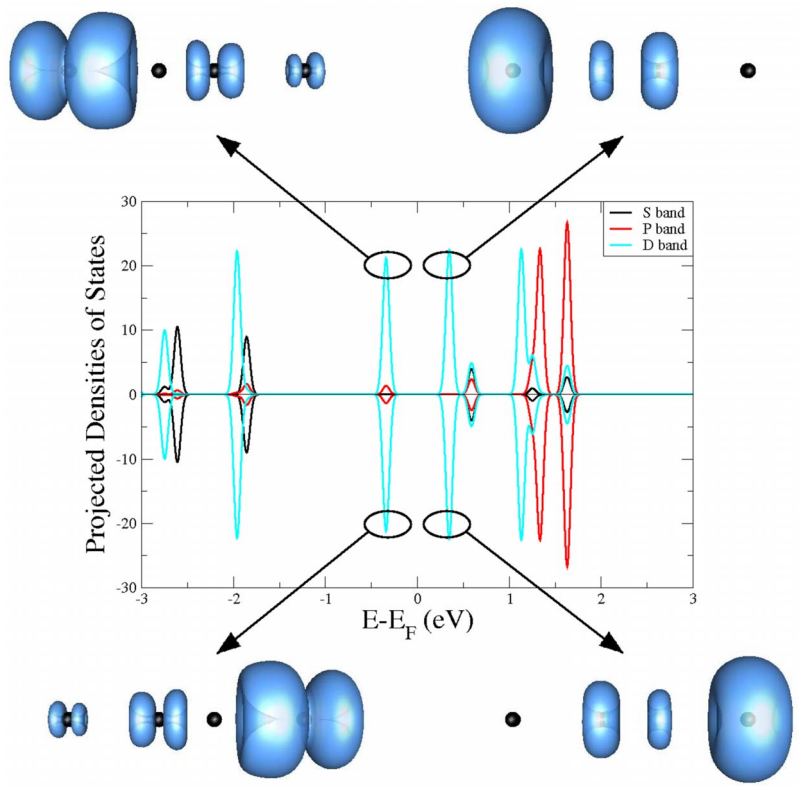

FIG. 4. (Color online) Orbital and spin projected densities of states for the ground-state AFM configuration of Mo_2Fe_2, together with the spin charge densities for the HOMO and LUMO states.

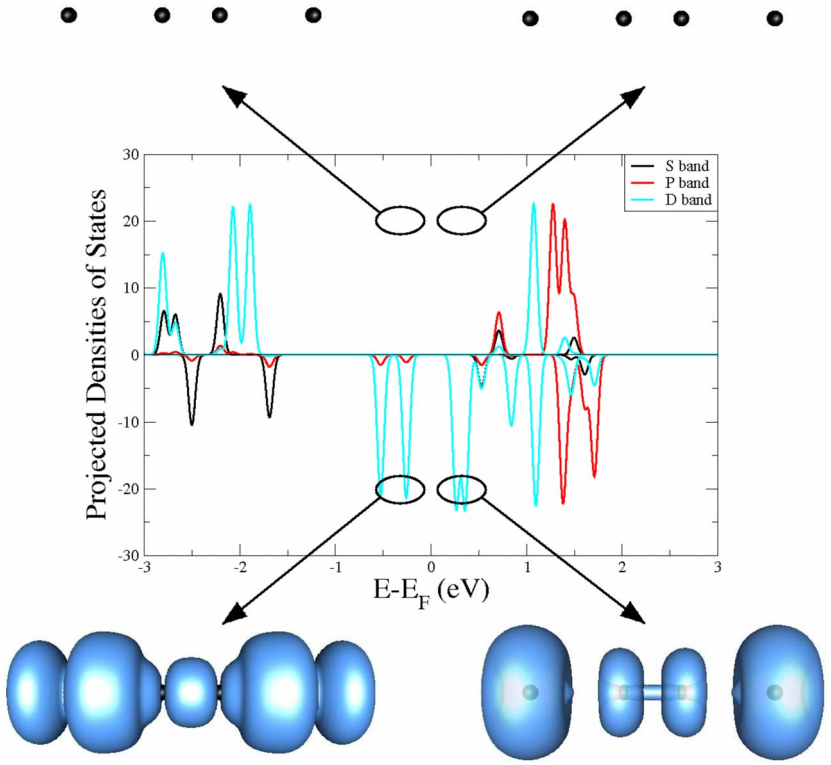

FIG. 5. (Color online) Orbital and spin projected densities of states for the FM configuration corresponding to the second lowest-lying isomer of Mo_2Fe_2, together with the spin charge densities for the HOMO and LUMO states.

substitutional doping by one and even two Fe atoms, above which a transition to the tetrahedral geometry of pure Fe_4 takes place. The cluster Mo_2Fe_2 is particularly interesting since its ground state and first-excited state essentially differ in the magnetic coupling between the two Fe atoms across a tightly bound Mo dimer. The equivalent to the IEC observed in sandwiches and multilayers is determined in this molecular magnet, whose electronic structure makes it a good candidate to be used either as a field sensor or as a spin valve in molecular spintronics. We believe that our work may stimulate further research to probe the applicability of these low-dimensional magnets as molecular spintronic units. Metallic nanostructures are susceptible to lose partially their electronic properties in environmental conditions different from the vacuum (e.g., under oxidation). In such case, and in order to functionalize them, efforts should be done to provide these molecular magnets with protections by encasing them into components which, besides preserving the desired properties, allow their attachment to the metallic leads. Experimental and theoretical work in this line will be of great interest.

ACKNOWLEDGMENTS

This work was supported by the Spanish Ministry of Education and Science in conjunction with the European Regional Development Fund under Grants No. FIS2008-02490/FIS and No. FIS2008-04894/FIS, the Dirección Xeral de I+D+I de la Xunta de Galicia under Grants No. INCITE08E1R206041ES and No. INCITE08PXIB206107PR, and the Junta de Castilla y León under Grant No. GR120. One of us (FAG) also acknowledges Grants No. PROMEP-SEP-CA230, No. CONACyT 2005-50650, and the computer sources from the Centro Nacional de Supercomputo from IPICyT, San Luis Potosi, Mexico.

[1] S. A. Wolf, D. D. Awschalom, R. A. Buhrman, J. M. Daughton, S. von Molnár, M. L. Roukes, A. Y. Chtchelkanova, and D. M. Treger, Science **294**, 1488 (2001).
[2] G.-H. Kim and T.-S. Kim, Phys. Rev. Lett. **92**, 137203 (2004).
[3] P. Grünberg, R. Schreiber, Y. Pang, M. B. Brodsky, and H. Sowers, Phys. Rev. Lett. **57**, 2442 (1986).
[4] S. S. P. Parkin, N. More, and K. P. Roche, Phys. Rev. Lett. **64**, 2304 (1990).
[5] M. N. Baibich, J. M. Broto, A. Fert, F. Nguyen Van Dau, F. Petroff, P. Etienne, G. Creuzet, A. Friederich, and J. Chazelas, Phys. Rev. Lett. **61**, 2472 (1988).
[6] G. Binasch, P. Grünberg, F. Saurenbach, and W. Zinn, Phys. Rev. B **39**, 4828 (1989).
[7] I. M. L. Billas, J. A. Becker, A. Châtelain, and W. A. de Heer, Phys. Rev. Lett. **71**, 4067 (1993).
[8] A. J. Cox, J. G. Louderback, S. E. Apsel, and L. A. Bloomfield, Phys. Rev. B **49**, 12295 (1994).
[9] A. Vega, J. Dorantes-Dávila, L. C. Balbás, and G. M. Pastor, Phys. Rev. B **47**, 4742 (1993).
[10] M. B. Knickelbein, Phys. Rev. B **75**, 014401 (2007).
[11] J. Bansmann, S. H. Baker, C. Binns, J. A. Blackman, J.-P. Bucher, J. Dorantes-Dávila, V. Dupuis, L. Favre, D. Kechrakos,

A. Kleibert, K.-H. Meiwes-Broer, G. M. Pastor, A. Perez, O. Toulemonde, K. N. Trohidou, J. Tuaillon, and Y. Xie, Surf. Sci. Rep. **56**, 189 (2005).
[12] R. Ferrando, J. Jellinek, and R. L. Johnston, Chem. Rev. (Washington, D.C.) **108**, 845 (2008).
[13] M. D. Morse, Chem. Rev. (Washington, D.C.) **86**, 1049 (1986).
[14] H. Cheng and L.-S. Wang, Phys. Rev. Lett. **77**, 51 (1996).
[15] C. Kohl and G. F. Bertsch, Phys. Rev. B **60**, 4205 (1999).
[16] D. Hobbs, G. Kresse, and J. Hafner, Phys. Rev. B **62**, 11556 (2000).
[17] W. Zhang, X. Ran, H. Zhao, and L. Wang, J. Chem. Phys. **121**, 7717 (2004).
[18] F. Aguilera-Granja, A. Vega, and L. J. Gallego, Nanotechnology **19**, 145704 (2008).
[19] J. M. Soler, E. Artacho, J. D. Gale, A. García, J. Junquera, P. Ordejón, and D. Sánchez-Portal, J. Phys.: Condens. Matter **14**, 2745 (2002).
[20] V. M. García-Suárez, C. M. Newman, C. J. Lambert, J. M. Pruneda, and J. Ferrer, J. Phys.: Condens. Matter **16**, 5453 (2004).
[21] J. P. Perdew, K. Burke, and M. Ernzerhof, Phys. Rev. Lett. **77**, 3865 (1996).
[22] N. Troullier and J. L. Martins, Phys. Rev. B **43**, 1993 (1991).
[23] L. Fernández-Seivane and J. Ferrer, Phys. Rev. Lett. **99**, 183401 (2007).
[24] T. Morisato, S. N. Khanna, and Y. Kawazoe, Phys. Rev. B **72**, 014435 (2005).
[25] R. C. Longo, E. G. Noya, and L. J. Gallego, Phys. Rev. B **72**, 174409 (2005).
[26] M. Kabir, D. G. Kanhere, and A. Mookerjee, Phys. Rev. B **75**, 214433 (2007).
[27] R. C. Longo, M. M. G. Alemany, J. Ferrer, A. Vega, and L. J. Gallego, J. Chem. Phys. **128**, 114315 (2008).
[28] T. He, Y. Gao, F. Zeng, and F. Pan, J. Phys. D **37**, 1 (2004).
[29] M. Di Ventra, S. T. Pantelides, and N. D. Lang, Phys. Rev. Lett. **84**, 979 (2000).